

Extensions of the Burst Generation Rate Method for Wider Application to Proton/Neutron-Induced Single Event Effects

Eugene Normand, *Member, IEEE*,

Boeing Information, Space & Defense Systems, Seattle, WA 98124-2499

Abstract

The Burst Generation Rate (BGR) method, originally developed to calculate single event upset (SEU) rates in microelectronics due to neutrons and protons, has been extended for wider application, allowing cross sections for both SEU and single event latchup (SEL) to be calculated, and comparisons to be made with measured data. The method uses the Weibull fit to accurately represent the behavior of the heavy ion SEU cross section. Proton SEU cross sections in RAMs, microprocessors and FPGAs are calculated, with agreement generally to within a factor of 2-3, and similar results are obtained for neutron cross sections for both cosmic ray and fission spectra. The BGR method is also modified to calculate cross sections for proton/neutron induced SEL. Agreement is generally good for SEL for most devices, but there are also limitations, since some very modern devices are shown to have unusually high susceptibility to SEL by protons/neutrons.

I. INTRODUCTION

The burst generation rate (BGR) method was developed by Ziegler at Lanford [1] to calculate the rate of single event upset (SEU) induced by protons and neutrons in silicon via the energy deposition from the resulting reaction products. Letaw and Normand developed the method further by incorporating both more recent and more accurate silicon cross section data, as well as the results of energy transport calculations [2]. Since then, two additional advances have been made, the use of the Weibull fit to accurately represent the continuous behavior of heavy ion SEU cross sections, and the reformulation of the method to calculate SEU cross sections, rather than SEU rates. The reformulation is important because measured proton and neutron SEU data are mainly available in the form of SEU cross sections and not as SEU rates. The first extension we show is incorporating the Weibull distribution in its differential, rather than its integral form.

In terms of comparisons with actual data, the first extension of the BGR method discussed in this paper is to compare BGR proton SEU cross sections against measured proton SEU cross sections for a variety of devices, random access memories (RAMs), microprocessors and field program-mable gate arrays (FPGAs). Several other methods are available to calculate proton-induced SEU cross sections by utilizing various kinds of SEU-related test data [3-5]. A comparison will be made with one of these methods, one that provides data on a large number of RAMs [3]. Because of the recent availability of measured SEU cross sections by fission neutrons [6], a

comparison of the BGR-calculated cross sections will also be made for this new kind of data, neutron-induced SEU cross sections from fission neutrons.

We will also show how the BGR method, in the SEU cross section format, can be extended to two other applications, calculating SEU cross sections for different spectra, and for single event latchup (SEL). Having measured proton/neutron SEU cross sections for one specified particle energy spectrum, the method can be used to calculate SEU cross sections for a different particle spectrum. In the case of monoenergetic proton beams of two different energies, this is straightforward using other calculational methods [3,7]. However, in the case of two neutron spectra, such as the atmospheric neutron spectrum and a 14 MeV neutron generator, at present only the BGR method can handle this case. Thus, using the BGR method, we will show how an SEU cross section measured with a 14 MeV neutron generator can be converted to an SEU cross section for the cosmic ray neutron spectrum.

Second, the BGR method can be modified to calculate cross sections for proton/neutron induced SEL. The key assumption required in this modification is that the silicon recoils created by interactions with the protons/neutrons must have a minimal range of $\sim 6 \text{ } \mu\text{m}$, before their energy deposition can be considered as contributing to latchup. This model was described previously [8], but in that case, it was applied to only a single device. In this paper the model is applied to a number of different device types, with generally good results, and observations about how some very modern devices appear to be much more susceptible to proton-induced SEL than previous devices.

Finally, we will extend the initial thrust of the BGR method toward calculating SEU rates. In this case we will apply the method to proton-induced SEU rates, providing a convenient way to calculate rates for the trapped proton flux for a given orbit via a simple equation and an accompanying BGR-related curve. This will approach will be illustrated for the Space Station orbit.

II. BGR Method

The BGR method was developed by Ziegler and Lanford to calculate the SEU rate induced by protons/neutrons interacting with a microelectronics device. The energy deposited by the recoils from particle (proton or neutron) reactions is what causes the upset, and the SEU rate is given by

$$\text{Up Rate} = C \dot{\mathbf{a}} \sum_i^N t \Delta \sigma_i \dot{\mathbf{O}} \text{BGR}(E_p, E_{ri}) \frac{dJ}{dE} dE_p \quad (1)$$

The following terms are defined: C is the collection efficiency, t is the collection depth (in μm), $\Delta \sigma_i = \sigma_i - \sigma_{i-1}$, where σ_i is the heavy ion SEU cross section for i th portion of curve, cm^2 , $\text{BGR}(E_p, E_{ri})$ is the burst generation rate, $\text{cm}^2/\mu\text{m}^3$, E_p is the energy of the incoming particle, MeV, E_{ri} is the i th recoil energy, ($E_{ri} = t \times 0.23 \times \text{LET}_i$, in MeV) and dJ/dE is the particle differential flux, particle/ $\text{cm}^2\text{-sec-MeV}$.

The key part of the method is the BGR function $\text{BGR}(E_p, E_{ri})$ which expresses the probability that an incident particle of energy E_p , interacting with atoms of a material such as silicon, will produce recoils having energy $\geq E_{ri}$. These functions have been calculated using the results of HETC (High Energy Transport Code [9]) calculations for neutrons ($E_p > 50$ MeV) in an infinite medium of silicon, or by using ENDF (Evaluated Nuclear Data Files [10]) neutron silicon cross sections along with reaction kinematics for $E_p < 20$ MeV. For $E_p > 50$ MeV, the neutron BGR functions are assumed to also apply to protons, and for $E > 100$ MeV, this is considered a good assumption which begins to lose its validity as the energy decreases below 100 MeV. The set of BGR functions for silicon that will be used is shown in Figure 1 [2] for various values of E_p and E_{ri} .

Another important part of the BGR method that has improved its overall accuracy, is the use of the Weibull fit to calculate the variation of the heavy ion SEU cross section, $\sigma_i = \sigma(\text{LET}_i)$, as a function of LET

$$\sigma_i = \sigma(L_i) = \sigma_0 \left\{ 1 - \exp\left\{-\left[\frac{L_i - L_0}{W}\right]^S\right\}\right\} \quad (2)$$

where the four Weibull parameters are: σ_0 is the asymptotic cross section (per bit or per device), L_0 is the LET cutoff and S and W are fitting parameters [7].

The BGR method also uses two specialized parameters, t , the collection depth (sometimes called the sensitive thickness), and C, the collection efficiency which accounts for the fact that not all the energy deposited by the energetic recoils within the collection volume lead to upsets.

In addition to representing the heavy ion SEU cross section well, another advantage of using the Weibull fit is that it provides the cross section as a continuous function of LET. Thus, the original form of the SEU rate, Eq (1), using the summation over LET (LET_i , $i=1, N$), can be replaced by an equivalent formulation based on the integration over LET,

$$\text{UpRate} = C t \dot{\mathbf{O}} \frac{ds}{dL} \dot{\mathbf{O}} \text{BGR}(E_p, E_r) \frac{dJ}{dE} dE dL \quad (3)$$

in which the differential form of the Weibull fit, ds/dL , can be used,

$$\frac{ds}{dL} = (S\sigma_0/W) \left(\left[\frac{L - L_0}{W} \right]^S - 1 \right) \times \left\{ \exp\left\{-\left[\frac{L - L_0}{W}\right]^S\right\} \right\} \quad (4)$$

instead of the integral form given in Eq (2).

As has previously been shown [12], another use of the BGR method is to provide an expression for evaluating the SEU cross section, rather than the SEU rate. This is achieved by simply removing the integration over energy E_p with the differential particle flux. Thus, we obtain the expression for the SEU cross section in the original formulation as a summation over LET_i values.

$$\sigma_p = \sigma(E_p) = C \dot{\mathbf{a}} \sum_i^N \text{BGR}(E_p, E_{ri}) t \Delta \sigma \quad (5)$$

or its equivalent formulation as an integral over LET, L.

$$\sigma_p = \sigma(E_p) = C t \dot{\mathbf{C}} \text{BGR}(E_p, E_r) ds/dL dL \quad (6)$$

III Proton SEU Cross Sections

To examine how good a job the BGR method, through either Eqs (5) or (6), does in calculating the SEU cross section, we compare the results of applying the method to SEU data for 18 RAM parts. These parts were tested with both heavy ions and protons, by a variety of researchers, and the SEU data, in terms of the Weibull parameters for the heavy ion cross section and the measured cross sections for the protons were selected and compiled by P. Calvel [3]. Calvel used these Weibull parameters in conjunction with his own method of calculating proton SEU cross sections, based on a pseudo-elastic scattering methodology and incorporated into his PROFIT (PROton FIT) code. Both PROFIT and the BGR method used a collection depth of 2 μm . The BGR method used $C=0.5$ for all the RAMs. PROFIT uses one free parameter, the average diffusion angle [3], which was between 40-70° for 13 of the RAMs, and more broadly in the range of 19-90° for all of the RAMs.

In Figure 2 we compare the proton SEU cross sections as measured by the test groups, and as calculated using the Weibull fits to the heavy ion SEU cross sections via the two methods, PROFIT code, and the BGR method. In general, both calculational methods give relatively similar agreement, and compared to the measured cross sections, the calculated values are off by less than a factor of 3 for all of the parts, and are within a factor of 1.6 for more than 60% of the parts. The worst agreement for the BGR method is a factor of 3 for part #9, and for PROFIT, a factor of 2.5 for part 18. Details of the SEU data for the 18 parts, including the Weibull parameters, are found in [3], as well as the order in which they are listed.

We also compare how well the BGR method works for other types of microelectronic devices, in this case the Motorola 68020 microprocessor and two Actel FPGAs. SEU cross sections induced by both heavy ions and protons have been measured for these parts, by Velazco et al in the 68020 [13] using three different programs/conditions, and by both NASA-GSFC [14-16] and Actel [17] in the Actel FPGAs. Table 1 summarizes the measured and calculated proton SEU cross

sections for these devices. The agreement is similar to that for the RAMs, i.e., generally within a factor of 2-3, except for the SORT test program with cache in the 68020, where the calculated values are too low by almost 5.

One of the features of the BGR method that should be reiterated is that it relies on only two extraneous parameters, t ,

the collection depth, and C , the collection efficiency. Based on our experience with the BGR method, we find that default values of $t = 2 \mu\text{m}$ and $C = 0.5$ work well for most devices. The $t = 2 \mu\text{m}$ applies to post-1990 devices, but for older devices with larger feature sizes, larger values of t should be used, e.g. for the IMS1601 SRAM first available in the mid 1980s, the optimum value of t is $5.5 \mu\text{m}$. [18].

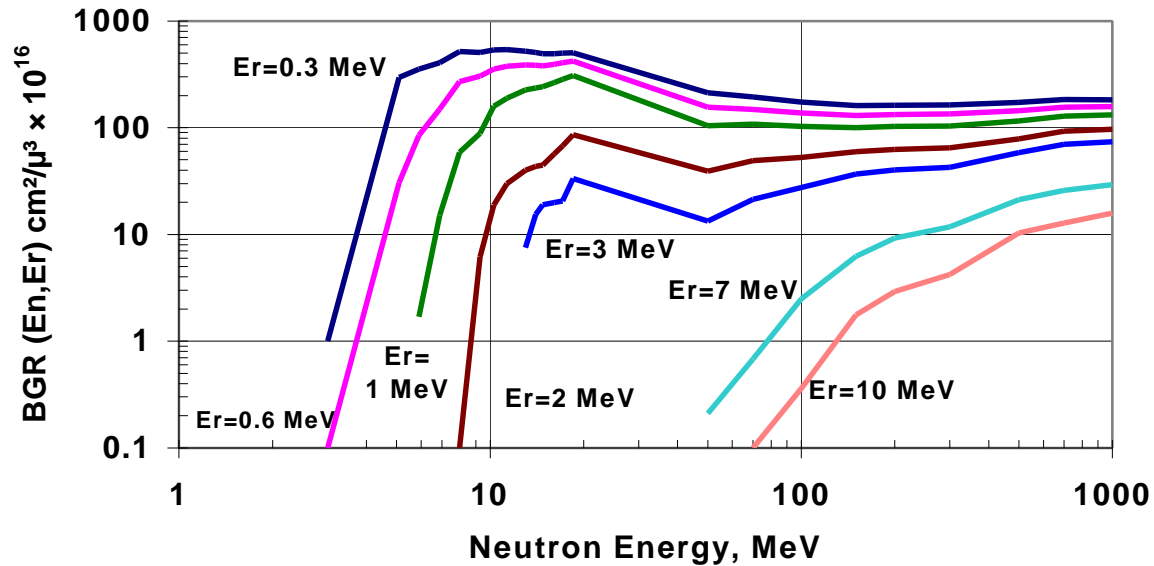


Figure 1 $BGR(E_p, E_r)$ Functions for Neutrons of Energy E_p Creating Recoils of Energy E_r

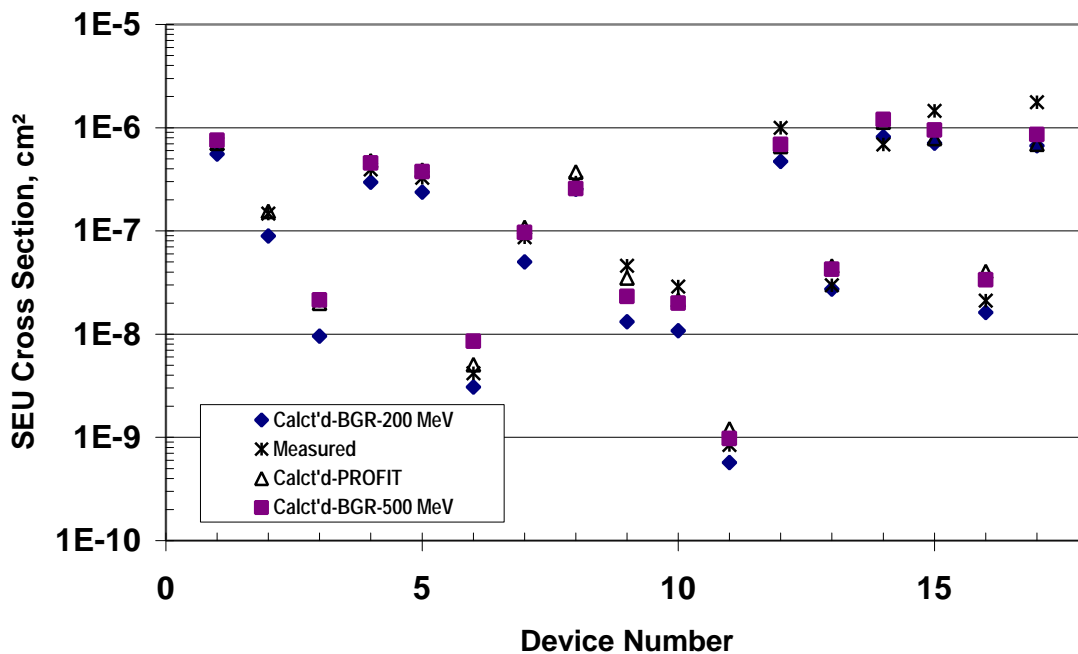


Figure 2 Comparison of Measured 200 MeV Proton SEU Cross Sections for 18 RAMs

Table 1 Proton-Induced SEU Cross Sections in Microprocessors and FPGAs, Measured and as Calculated by BGR Method

Device	Measured		BGR Calculation		Comments	Data Refs
	Ep, MeV	X-Sctn, cm ²	Ep, MeV	X-Sctn., cm ²		
68020	45	1.3E-08	50	2.2E-09	μprocessor, per dev, SORT, w/ cache	13
"	70	1.2E-08	100	2.4E-09	μprocessor, per dev, SORT, w/ cache	13
"	100	1.1E-08	200	2.8E-09	μprocessor, per dev, SORT, w/ cache	13
"	200	1.2E-08			μprocessor, per dev, SORT, w/ cache	13
"	100	2.5E-10	100	2.2E-10	μprocessor, per dev, SORT, no cache	13
"	200	1.1E-09	200	3.3E-10	μprocessor, per dev, SORT, no cache	13
"	70	5.2E-10	50	5.0E-10	μprocessor, per dev, REG, w/ cache	13
"	100	1.2E-09	100	9.0E-10	μprocessor, per dev, REG, w/ cache	13
"	200	2.0E-09	200	1.5E-09	μprocessor, per dev, REG, w/ cache	13
1020	196	1.8E-15	200	4.0E-15	Actel FPGA, per flip/flop	14
1280	196	1.3E-13	200	4.0E-13	Actel FPGA (1μ, 5V) per flip/flop	15
1280	196	1E-13	200	4.0E-13	Actel FPGA, (0.8μ, 4.5V) per f/f	16
1280	196	3.5E-13	200	4.0E-13	Actel FPGA, (0.6μ, 4.5V) per f/f	16
1280	150	0.2-6 E-13	200	4.0E-13	Actel FPGA, per flip/flop	17
1280	90	1.5-6 E-13	100	2.3E-13	Actel FPGA, per flip/flop	17
1280	50	0.9-3E-13	50	1.0E-13	Actel FPGA, per flip/flop	17

IV Neutron SEU Cross Sections

We have previously reported on a number of devices that were tested for SEU in neutron beams, rather than with proton beams [19, 20]. In most cases, the neutron beam used was the Weapons Neutron Research (WNR) facility at Los Alamos National Laboratory. This neutron beam has been found to be very useful because it simulates the cosmic ray neutron spectrum so well [12,19]. Therefore, SEU cross sections measured in the WNR beam are applicable to RAM memories and other devices used in avionics at aircraft altitudes [12] and in large computer systems on the ground [20].

Table 2 contains WNR neutron SEU cross sections, both measured and calculated. Because the cosmic ray neutron spectrum is not monoenergetic, the calculated SEU cross sections were obtained using Eqs (1) or (3), rather than Eqs. (5) or (6). For this spectrum, the integral of the BGR (E_p , E_r) with the differential flux, dJ/dE , is carried out over E_p , and the resulting function, $BGR_{int}(E_r)$ is shown in Figure 3 as a function of E_r .

$$BGR_{int}(E_r) = \int_{E_p} BGR(E_p, E_r) dJ(E_p) / dE dE_p \quad (7)$$

The differential neutron flux used is

$$dJ/dE = 0.346E^{-0.922} \times \exp[-0.01522(\ln E)^2] \text{ n/cm}^2 \text{ sec MeV} \quad (8)$$

which is based on our fit [18] to the airborne measurements by Hewitt [21] and correlated to conditions of 40,000 ft altitude and 45° N latitude. Thus, the units of $BGR_{int}(E_r)$ in Figure 3 for the cosmic ray neutrons is $1/\mu\text{m}^3$, since the normalized version of the spectrum was used [dJ/dE of Eq. 8 divided by

the integral flux of 1.6 n/cm^2 ($E > 10 \text{ MeV}$)]. The calculated atmospheric neutron cross section is obtained by using the $BGR_{int}(E_r)$ function shown in Figure 3 in Eqs. (1)/(3).

Table 2 Comparison of SEU Cross Sections Induced by the WNR Spectrum, Measured and Calculated by BGR Method

Device	Measured WNR SEU Cross Section, cm ² /bit	Calculated BGR SEU Cross Section for WNR, cm ² /bit
IMS1601	4E-13	9.5E-13
TC514400	1.2E-13	1.2E-13
TMS44100	8.6E-14	1.2E-13
IDT71256	6.5E-14	1.1E-13
MCM6246	1.25E-14	2E-14
87C196	4.8E-10*	9.1E-10*

* SEU Cross section as cm²/device

There are several other examples of neutron sources with distinct high energy (> 1 MeV) spectra as given in [2], such as the PuBe source and pure fission source. In Figure 3 we also include the $BGR_{int}(E_r)$ functions for the fission neutron spectrum. The fission spectrum is of special interest because of some recent SEU measurements made in devices using the SPR reactor [6]. The neutron spectrum of the Sandia Pulsed Reactor (SPR) reactor, which extends over 9 orders of magnitude (.01 eV-10 MeV), can be altered by the inclusion of various neutron absorbers within the reactor.

In [6], six SRAMs were tested and five of them had SEUs induced primarily by the thermal neutrons. However, for one SRAM essentially all of the SEUs were induced by the fission

neutrons ($E > 1$ MeV), and for three others an appreciable portion of the SEUs were attributable to the fission neutrons. Thermal neutrons induce SEU through the $n\text{-B}^{10}$ reaction that results in an alpha particle (He^4 , 1.48 MeV maximum energy) and a Li^7 particle (0.85 MeV maximum energy). The distribution of B^{10} in the die is non-uniform and complex (it may be in the borophosphosilicate glass layer, the P-well dopant or chemically diffused throughout the silicon), and so energy deposition by the He^4 and Li^7 is complex and will not be dealt with here. In principle the BGR method could be applied to the $n\text{-B}^{10}$ reaction to obtain a more rigorous treatment of the energy deposition via this reaction.

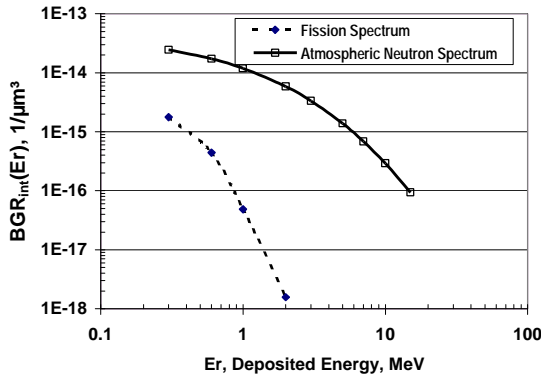


Figure 3 $BGR_{int}(E_r)$ for Fission and Atmospheric Neutron Spectra

Therefore, for purposes of this paper, we look only at the three SRAMs in [6] for which we can quantify the SEU cross section due to fission neutrons. For each of the three SRAMs (all are 1Mbit), at least 300 SEUs were induced by fission neutrons during the combined tests in the SPR reactor with up to four different spectra. This data is summarized in Table 2. Also included in the table is data on a microprocessor that was also tested in the SPR reactor. The microprocessor exhibited one SEU when exposed to the mainly fission spectrum [22] and none when exposed to the primarily thermal neutron spectrum. We use the $BGR_{int}(E_r)$ curve for the fission spectrum (normalized to 1 n/cm^2) in Figure 3, along with Eqs (1)/(3) to calculate the SEU cross section of the SRAMs and the microprocessor.

The results of the measured and calculated SEU cross sections from fission neutrons for the four devices are listed in Table 3. Since we do not have the Weibull parameters for the specific SRAMs and microprocessor that were tested in the SPR reactor, similar surrogate devices for which Weibull parameters are available were used in the BGR calculations. These devices are also listed in Table 3. Three different SRAMs with known Weibull parameters were used, two from Calvel [3] and one a 1Mbit SRAM. The surrogate SRAMs were chosen somewhat arbitrarily, only for the purpose of providing the behavior of the per bit heavy ion SEU cross section as a function of LET. In Table 3 we see that the result of using the Weibull fit for these three surrogate SRAMs is calculated fission neutron SEU cross sections that differ by

about a factor of 3. This indicates that the low LET behavior of the heavy ion SEU cross section fit for the three SRAMs are relatively similar, since the low energy fission neutrons (< 10 MeV) produce low LET recoils.

The measured SEU cross sections in each SRAM varied by about a factor of 2, depending on which SPR spectrum was used. Therefore, considering this variation in the measured SEU cross sections, the agreement with the fission neutron SEU cross sections as calculated by the BGR method is rather good, within about a factor of 2. This assumes that the heavy ion SEU cross sections for the tested and surrogate SRAMs are similar, but if they differ significantly, the factor of 2 could be much higher (see section V discussion). For the microprocessor the agreement is poorer, but since a single SEU event was measured, there is large uncertainty in this measured value.

Table 3 SEU Cross Sections Due to Fission Neutrons, Measured at SPR Reactor and Calculated by BGR Method

Device Tested at SPR	Total # SEUs due to Fission Neutrons	Msr'd SEU X-Sct'n at SPR, cm^2/bit	BGR Calc'd SEU X-Sct'n, cm^2/bit	Surrog Device w/ Weib params
SRAM A	~1700	2.2-4E-16	1.7E-16	MCM622 6B
SRAM B	~400	5-10E-17	5E-17	HM65656
Sharp SRAM	~300	5.5-11E-17	1.3E-16	62256R
μprocessor*	1	1.E-13	6.0E-13	XC68302

*SEU cross section is per device

In Table 3 we tabulate some measured and calculated SEU cross sections for the WNR/cosmic ray neutron spectrum. The calculated cross sections were obtained using the BGR method [19,20]. Not in every case were heavy ion cross sections available for the same device as was exposed to the WNR beam, so in those cases related surrogate devices were used for which the Weibull parameters are available [19,20]. In this case the surrogate RAMs were chosen to be as close to the devices tested in the WNR as possible, e.g., for the TC514400 and CY7C195 RAMs tested, we used Weibull parameters for the related RAMs TC514100 and CY7C185 [20].

V SEU Cross Sections for Different Particle Spectra

The BGR method can be used to convert a measured SEU proton/neutron cross section made with one energetic particle spectrum to that for a different particle spectrum. A good example of this is for neutrons with the two different spectra, and two of the most commonly used spectra are those of 14 MeV (monoenergetic) and cosmic ray neutrons (continuous over energy). In Table 4 we compare the neutron SEU cross sections in SRAMs for the cosmic ray spectrum as directly

measured in the WNR beam [20], and as calculated with the BGR method using measured 14 MeV SEU cross sections. There are actually two ways to do this. Both require the use of a Weibull function for a surrogate device (Dev_s) to represent the heavy ion SEU cross section behavior of the device of interest (Dev_i), but normalized by means of the 14 MeV SEU cross sections (for Dev_s and Dev_i). We recognize that although we need the complete Weibull function description of the Dev_i in order to use the BGR method, we can modify the process in one of two convenient ways, by varying C or σ_o , through normalization with the 14 MeV SEU cross sections. Thus we assume that the shape of the heavy ion SEU cross section curve is essentially the same for the two devices, Dev_s and Dev_i , which is equivalent to using the set of three Weibull parameters L_o , W and S for a related surrogate device, Dev_s .

This assumed similar behavior of the heavy ion SEU cross section definitely applies to SRAMs. Scores of SRAMs have been tested for SEU with heavy ions, and invariably the cross section curve as a function of LET has a very similar shape for all of the commercial devices (SEU-hardened devices are excluded). This means that all of the heavy ion SEU curves are essentially parallel, differing by a constant factor except at the very lowest values of LET where the cross section values merge. The heavy ion SEU cross sections for about 15 different SRAMs in several figures of [35] shows this effect

quite clearly. Although the asymptotic cross section, σ_o , for the SRAMs in [35] differ by as much as four orders of magnitude, all of the curves have essentially the same shape.

To implement this application of the BGR method, the BGR_{int} (Er) function for the cosmic ray neutron spectrum is used. Six parameters are needed to calculate the SEU cross section with the BGR method, the four Weibull parameters and C and t. We fix four of these, t (2 μ m) and Weibull parameters L_o , W and S as discussed above, and for the remaining pair of parameters C and σ_o , one is fixed and the other normalized via the 14 MeV SEU cross sections. In the first approach, the σ_o of Dev_s is used as the σ_o for Dev_i and C is varied to obtain agreement with the measured 14 MeV SEU cross section. This normalized value of C is used to calculate the SEU rate and cross section for the cosmic ray neutron spectrum. In the second approach, the standard C=0.5 is used, and σ_o for Dev_s is normalized by means of the 14 MeV SEU cross sections to obtain the σ_o for Dev_i . This normalized value of σ_o is then used with the BGR functions based on the cosmic ray neutron spectrum to obtain the cosmic ray or WNR SEU cross section. Two different SRAMs were used as Dev_s , IDT71256 and MCM6246, to provide the Weibull parameters for the heavy ion SEU cross sections in order to show the broad applicability of this method. The Weibull parameters are IDT71256: $\sigma_o=$

Table 4 Calculated Cosmic Ray Neutron SEU Cross Sections (BGR Method w/ 14 MeV SEU X-Sections)

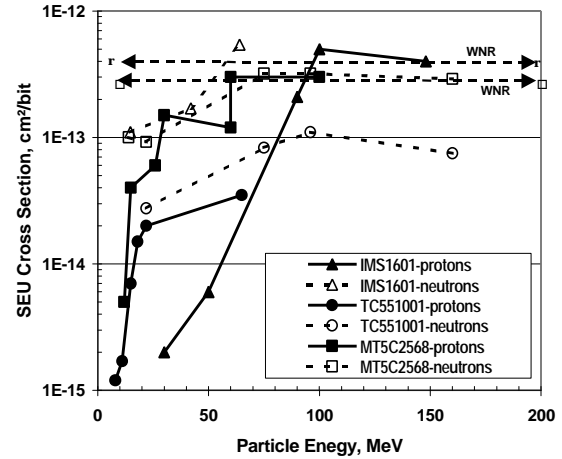
SRAM	Msr'd 14 MeV X-Sct'n, cm ² /bit	Msr'd WNR X-Sct'n, cm ² /bit	C/ σ_o values used w/ Weibull	BGR Calct'd WNR X-Sct'n, cm ² /bit	Ratio, WNR, Calctd/Msr'd
Based on using Weibull for the IDT71256, $\sigma_o=7.4E-7$					
IDT71256	2.7E-14	7.8E-14	0.21/7.4E-7	4.98E-14	0.64
IMS1601	1.1E-13	4.0E-13	0.85/7.4E-7	2.03E-13	0.51
CY7C199	1.1E-13	5.1E-13	0.85/7.4E-7	2.03E-13	0.40
MT5C2568	1.0E-13	3.2E-13	0.77/7.4E-7	1.84E-13	0.58
MCM6246	8.2E-15	1.3E-14	0.06/7.4E-7	1.51E-14	1.16
Based on using Weibull for the IDT71256, $\sigma_o=7.4E-7$					
IDT71256	2.7E-14	7.8E-14	0.5/7.4E-7	1.19E-13	1.52
IMS1601	1.1E-13	4.0E-13	0.5/3E-6	4.83E-13	1.21
CY7C199	1.1E-13	5.1E-13	0.5/3E-6	4.83E-13	0.95
MT5C2568	1.0E-13	3.2E-13	0.5/2.7E-6	4.39E-13	1.37
MCM6246	8.2E-15	1.3E-14	0.5/2.2E-7	3.60E-14	2.77
Based on using Weibull for the MCM6246, $\sigma_o=5.3E-8$					
IDT71256	2.7E-14	7.8E-14	1.28/5.3E-8	5.04E-14	0.65
IMS1601	1.1E-13	4.0E-13	5.2/5.3E-8	2.05E-13	0.51
CY7C199	1.1E-13	5.1E-13	5.2/5.3E-8	2.05E-13	0.40
MT5C2568	1.0E-13	3.2E-13	4.7/5.3E-8	1.87E-13	0.58
MCM6246	8.2E-15	1.3E-14	0.39/5.3E-8	1.53E-14	1.18
Based on using Weibull for the MCM6246, $\sigma_o=5.3E-8$					
IDT71256	2.7E-14	7.8E-14	0.5/1.8E-7	6.46E-14	0.83
IMS1601	1.1E-13	4.0E-13	0.5/7.1E-7	2.63E-13	0.66
CY7C199	1.1E-13	5.1E-13	0.5/7.1E-7	2.63E-13	0.52
MT5C2568	1.0E-13	3.2E-13	0.5/6.5E-7	2.39E-13	0.75
MCM6246	8.2E-15	1.3E-14	0.5/5.3E-8	1.96E-14	1.51

7.4E-7, $L_0= 2.66$, $W= 16.4$, $S= 1.19$ and MCM6246: $\sigma_0= 5.3E-8$, $L_0= 1.1$, $W= 5.45$, $S= 6.88$. As seen in Table 4, the agreement between the calculated cross sections is quite similar for both sets of Weibull parameters for both approaches, i.e., varying C or varying σ_0 .

The agreement with the measured WNR cross sections is in most cases < 2 , but more generally within a factor of 3. This is an important feature, because the Weibull fit for a specific part may not be available, but Weibull parameters for related parts may be used in its place in most cases, but this method cannot be applied universally. A device with a relatively high 14 MeV neutron SEU cross section will also have relatively high WNR and heavy ion SEU cross sections, the different SEU cross sections being approximately proportional. The BGR method, through both of the approaches that were evaluated, allows the proportionality factor between the SEU cross sections for the two neutron spectra to be calculated. The proportionality factor is largely driven by the behavior of the heavy ion SEU cross section at low LETs (< 10 MeV-cm²/mg), which appears to be similar for the vast majority of SRAMs that have been tested. However, if an SRAM is encountered for which the heavy ion SEU cross section behavior is significantly different, e.g., those with cross-coupled resistors, the method will not work nearly as well.

It is also appropriate to discuss the issue of the use of the BGR functions for the two main categories of spectra, neutrons and protons. As indicated previously, the BGR functions used in this paper were derived only on the basis of neutron interactions in silicon, but they are also being used for predicting SEU induced by protons. We had indicated that for $E > 100$ MeV, this is considered a good assumption, but it begins to lose its validity as the energy decreases below 100 MeV. To examine this assumption in greater detail, we have compiled proton and neutron SEU cross sections at lower energies for four different SRAMs, and compare them in Fig. 4. The four SRAMs are the IMS1601 (64K, proton data from [23], neutron data from [18]), the Toshiba TC551001 (1M, proton data from [24], neutron data from [25]), the NEC D431000 (1M, proton data from [24], neutron data from [25]) and the Micron MT5C2568 (non-LCRP, 256K, proton data from [24], neutron data from [25] and Table 4). The Toshiba and NEC SRAMs have such similar SEU responses to both protons and neutrons that only the Toshiba data is plotted in the figure. Fig. 4 clearly shows the validity of the assumption that for $E > 100$ MeV, the protons and neutrons have essentially the same SEU effect in microelectronics.

Fig. 4 also shows that for newer devices like the Toshiba, NEC and Micron SRAMs, the devices' SEU response to both protons and neutrons is very similar down to energies as low as 20 MeV. Thus for current devices, application of the neutron-based BGR functions to proton environments appears to be warranted down to energies of about 20 MeV. However, below 20 MeV, the proton SEU cross section decreases very



Fi

Figure 4 Comparison of Proton and Neutron SEU Cross Sections as Function of Particle Energy

rapidly with energy, which is not true for neutrons, and so use of the BGR functions will give an overly conservative estimate of the SEU response. This has been explained as the retardation effect of the Coulomb barrier with these relatively low energy protons. However, Figure 4 also shows that for an older part like the IMS1601, below about 80 MeV, the proton SEU cross section decreases much more rapidly than the neutron SEU cross section. For such parts, use of the neutron-based BGR functions of Fig. 1 for a proton environment could entail an SEU response that is overly conservative by at least an order of magnitude.

One explanation for the apparent good agreement between protons and neutrons in SEU response for newer SRAMs down to 20 MeV relates to the very small size of the sensitive volume in these devices. The smaller the volume, the higher the probability that only those recoils with the shortest ranges will be contributing to the energy deposition that results in SEU. One approach to analyzing this is through another set of BGR functions that have also been calculated with the LAHET code for both neutrons and protons [19] (infinite medium) for $E_p \geq 50$ MeV. These BGR functions are similar to those shown in Figure 1, but the output gives the distribution of recoil energy by ion. These LAHET BGR functions are higher than those of Fig. 1, with those for neutrons being higher than those for protons. This agrees with the SEU cross sections in Fig. 4, and appears to be due to the smaller contribution of recoils from elastic scattering by protons compared to neutrons because the reaction is more forward peaked. Looking at these BGR functions for E_p of 50 MeV, we find that for recoils with $E < 2.5$ MeV for ions F through Si, all the ions have ranges $< 2.4 \mu\text{m}$. Thus in a small sensitive volume, e.g. $1 \mu\text{m} \times 1 \mu\text{m} \times 2 \mu\text{m}$, that has a maximum path length of $2.45 \mu\text{m}$, a large fraction of the energy of such recoils will be deposited within the sensitive volume. For older devices with larger sensitive volumes (the collection depth of the IMS1601 was found to be $5.5 \mu\text{m}$ [18]), recoils with longer ranges and higher energies will also be able to contribute to the energy deposition leading

to SEU. Having BGR functions calculated for protons for $E < 50$ MeV would allow energy deposition to be evaluated in greater detail.

For the IMS1061, the proportion of protons with energies < 80 MeV, compared to those with $E_p > 80$ MeV, would determine just how conservative the SEU estimate using the BGR functions is, and this depends on the specific proton environment. Finally, SEU data for the WNR neutron spectrum is also shown in Fig. 4, and using 10 MeV as an effective SEU cutoff for neutrons, ~60% of the WNR neutrons have $E > 80$ MeV. Thus the WNR neutron SEU cross sections are similar to the monoenergetic proton and neutron SEU cross sections for $E > 100$ MeV to within about a factor of 2.

VI Proton SEU Rates in Space

The same approach regarding SEU rates can also be applied to orbits in space for which there is a unique proton spectrum, such as that due to the trapped belt protons. For low earth orbits, these proton spectra are calculated by averaging over a number of days of individual orbit trajectories in order to obtain a daily averaged spectrum. Typical spectra are discussed in [26] and can be obtained using computer codes such as SPACE RADIATION [27]. In addition, the shielding around a location of interest can attenuate the flux resulting in a modified spectrum. As a base case we have used the proton spectrum for a 500 km circular orbit at 52° inclination and shielded by 500 mil of aluminum [28]. The integration over E_p indicated in Eq (7) was carried out and the resulting curve of BGR_{int} as a function of E_r is shown in Figure 5. Because the differential proton spectrum is given in units of $p/cm^2\text{-day-MeV}$, BGR_{int} is in units of $(\mu m^3/day)$. Combining Eqs (3) and (7) the resulting proton SEU rate is then given by

$$SEURate = Ct \int_{L_0}^{\infty} dJ / dL BGR_{int}(0.23tL) dL \quad (9)$$

To demonstrate how this method works, we would like to compare measured proton-induced SEU rates against those calculated through Eq. 9 and Figure 5. This is difficult because the BGR_{int} in Figure 5 is for the Space Station orbit, and most satellites that have SEU data are in much different orbits. Nevertheless, we were able to find two sources of SEU data in spacecraft with measured SEU rates. These are for the Space Shuttle and the MIR station, and the data are summarized in Table 5.

SEUs in the general purpose computers (GPCs) were measured during Shuttle flights [29], and flight STS-48 is of particular interest because its orbit was 540 km, 57° , which is quite similar to that of Space Station. SEUs due to the protons in the 64K SRAM IMS1601 within the GPCs were identifiable because they occurred when traversing the South Atlantic Anomaly. Similarly, in [30] SEU rates are reported for parts used in the EXEQ (Equivalence Experiment) experiment that was flown on the MIR station for 516 days. Many SEUs (587) were measured in the twelve HM65756 SRAMs and two were

measured in the MC68020 microprocessor. From the data given in [30], the average proton-induced upset rate in SAA for the HM65756 SRAMs can be calculated (from the timing distribution of the SEUs, we see that ~15% of all upsets occur while in the SAA). The MIR orbit which, at 350 km, 52° , is similar, although lower than that for Space Station (proton flux reduced by about 5). The SEUs in the MC68020 are most likely due to cosmic rays and not protons, so in Table 5 we compare the BGR SEU rate in the microprocessor against the values calculated using laboratory data [30].

Table 5 shows that the BGR method gives fairly good results when compared to the measured proton SEU rates distribution in [29], and for the 1/5 lower proton fluxes for

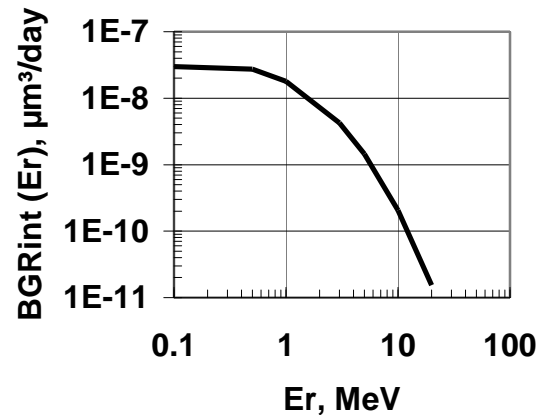


Figure 5 $BGR_{int}(E_r)$ for Trapped Proton Spectrum in 500 km, 52° Inclination Orbit

these two spacecraft. In obtaining the BGR SEU rates we used $C=0.5$ and $t = 2 \mu m$ for all the devices, and the specific Weibull parameters are listed in the table. Since the BGR_{int} function in Fig. 5 is for the Space Station shielding and orbit, we had to account for the additional shielding afforded by the Space Shuttle, as given by the shielding the MIR orbit. The good agreement in the SEU rate for GPC appears to be somewhat fortuitous because the SRAM involved, the IMS1601, has already been shown to have a much lower SEU susceptibility to protons than neutrons for $E < 80$ MeV, and the BGR functions are based on neutron responses. However, the significant amount of shielding involved reduces this effect substantially, e.g., for the Space Station orbit with 500 mils of Al, the total integral flux ($E > 10$ MeV) is $1.6E6 p/cm^2\text{-day}$, and the $E > 80$ MeV flux is $\sim 1E6 p/cm^2\text{-day}$. Thus almost 60% of the protons have energies > 80 MeV, whereas in the unshielded case, only 33% of the protons have energies > 80 MeV. Furthermore, for the GPCs on Shuttle, about 70% of the shielding is $> 1''$ Al. The Weibull parameters are IMS1601: $\sigma_0 = 0.66$, $L_0 = 0.93$, $W = 12.8$, $S = 1.88$; HM65656: $\sigma_0 = 1.25$, $L_0 = 1.1$, $W = 10$, $S = 0.78$; 68020: $\sigma_0 = 0.01$, $L_0 = 1.2$, $W = 10.35$, $S = 2.04$.

Table 5 Proton-Induced SEU Rates in Space, Measured and Calculated with BGR Method

Device/ Spacecraft	Orbit	Meas'd SEU Rate	BGR Calculated Rate
IMS1601/ Shuttle	540 km/ 57° (STS- 48)	5/GPC- day	8/GPC-day
HM65756/ MIR	350km/ 52°	.014/dev- day	0.03/dev-day (HM65656 [3])
MC68020/ MIR	350km/ 52°	2E-4/dev- day (calcl't'd)	5E-4/dev-day (Reg. Test w/cache)

VII Proton-Induced Single Event Latchup

The modifications needed to adapt the BGR method to the situation of single event latchup (SEL), have been previously described [8]. It is basically a fairly simple model constructed to incorporate the key assumption that the silicon recoils created by interactions with the protons/neutrons must have a minimum range in this case $\sim 6 \mu\text{m}$, before their energy deposition can be considered as contributing to latchup. Thus for each recoil characterized by a single atomic number Z , simplified LET-energy-range relationships are used to determine the range of the recoil, and those with a range $<$ the minimum $6 \mu\text{m}$, do not contribute to the modified BGR function that was developed for this application. Thus the collection depth, t , has more requirements in this model compared to the SEU model. For latchup, t specifies the minimum range of the recoils for their energy deposition to contribute, in addition to the depth of the collection volume. Once the recoils deposit their energy over a $6 \mu\text{m}$ path length, this energy, $\text{LET} \times t$, contributes to latchup, hence $C=1$.

In the original model, the requirement on long-ranged recoils was derived from heavy ion SEL tests carried out on the CY7C261 covered with varying thicknesses of aluminum foils [8]. As the foil thickness increased, the SEL cross section decreased, and eventually disappeared when covered with 25 μm of Al. The ion started out with a LET of 26 $\text{MeV}\cdot\text{cm}^2/\text{mg}$ and range of 38 μm , and after going through the 25 μm of Al, the LET was 30 $\text{MeV}\cdot\text{cm}^2/\text{mg}$ and the range 10 μm . The LET was large enough to cause latchup but the range was not. Thus, to sustain latchup, a minimum range of $\sim 10 \mu\text{m}$ is required entering the die, and when the 1-3 μm passivation layer is taken into account, this reduces to a minimum range of 6-10 μm within the die [8]. For generic application, we conservatively take this to be 6 μm . Thus, the energy deposition by the majority of the recoils, which have ranges in silicon of $< 6 \mu\text{m}$, does not contribute to latchup. Further, the modified BGR functions that we use are for 200 MeV protons, and are derived from calculations with LAHET (Los Alamos version of HETC) that are based on energy deposition within a $10 \times 10 \times 2.5 \mu\text{m}^3$ sensitive volume.

The modified BGR functions for a proton energy of 200 MeV are shown in Figure 6 as a function of E_r . We have applied

this BGR model to seven parts for which both heavy ion and proton SEL cross section data are available, and the results are tabulated in Table 6. As was the case with SEU, it is vital to have a relationship for the heavy ion SEL cross section as a function of LET, and again the Weibull fit is used for this, in order to implement this model. The source of the data for these parts is also included in the table. The Table 6 results show that the modified BGR method, despite its overall simplicity, works relatively well for five of the seven parts in being able to predict proton induced SEL cross sections using only heavy ion SEL cross section data. However, for the K-5 processor and the Motorola DSP96002, the method significantly underpredicts the proton SEL cross section, being off by about a factor of 300 for the K-5 and 20 for the DSP.

In [32] it was noted that the SEL behavior of the K-5 processor was distinctly different from that of other devices, having a very shallow epitaxial structure. It was further shown in [32] that the effective charge collection depth in the K-5 was much smaller, $\sim 25\text{-}30\%$ of that in the more typical devices. If we apply this effect to our simplified model, we obtain a BGR function based on recoils having ranges $> 2 \mu\text{m}$ (rather than $6 \mu\text{m}$). When this modified BGR function (range $> 2 \mu\text{m}$) is used, the BGR calculated proton SEL cross section is in good agreement with the measured value, as shown in Table 6. In Figure 6 modified BGR functions for 200 MeV protons are shown based on the energy deposition contributing to SEL when the recoil range in silicon exceeds several different values ($2 \mu\text{m}$, $4 \mu\text{m}$ and $6 \mu\text{m}$). Based on the data in Table 6, it appears that while $6 \mu\text{m}$ may be the appropriate minimum range for previous parts that are prone to proton-induced SEL, for some recent parts that undergo proton SEL, the energy deposition occurs over a shorter distance and the proton SEL cross section is much higher. Thus for the Motorola DSP96002, using the $6 \mu\text{m}$ minimum range gives rather poor agreement with the measured SEL cross section, however using a $4 \mu\text{m}$ minimum range with the BGR model gives fairly good agreement.

The magnitude of the proton SEL cross section seems to be the indicator of whether the original $t=6 \mu\text{m}$ recoil range requirement applies or not. Empirically, it appears that if the proton SEL cross section is $> 1\text{E-}9 \text{ cm}^2$, the original model is not able to predict the proton SEL response very well, and a smaller value of t is needed to account for greater energy deposition. This may be an over simplification, since it is not based on specific design features leading to increased sensitivity to SEL like the more accurate model [26]. However it is based on data from O'Neill and Culpepper [33] who indicate that in their proton SEE testing over the last two years, the four parts that experienced SEL all had cross sections $> 1\text{E-}9 \text{ cm}^2$. Of these four, only one, the DSP96002, is included in Table 6 because it is the only one that also has heavy ion SEL cross section data.

A more elaborate method has been developed for dealing with proton-induced SEL [32], and it is able to calculate a SEL cross section in good agreement with the measured value for

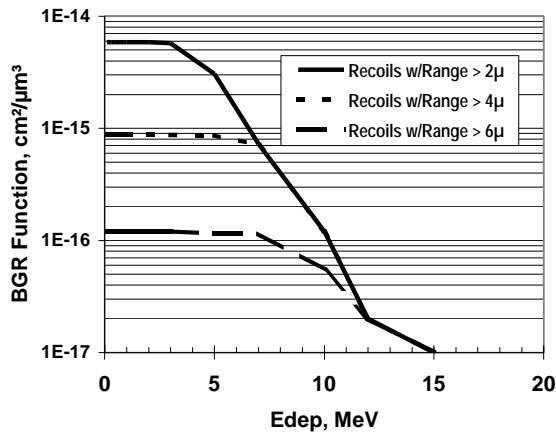


Fig 6. Modified BGR Function for Latchup Calculation (200 MeV Protons, Energy Deposition Depends on Recoils Range)

Table 6 Measured/ Calculated Proton SEL Cross Sections

Device	Meas'd Proton SEL X-Section, cm ²	BGR Calct'd Proton SEL X-Section, cm ²	Re- marks	Ref. for Data
HM65162	1.4E-10	1.4E-10		31
NEC-4464	1.8E-10	1.5E-10		32
K-5	6.6E-9	2.2E-11	t=6μm	32
K-5	6.6E-9	4E-9	t=2μm	32
LSI-64811	1.7E-11	6E-12		32
LCA200K	1.4-4.1E-11	7.6E-11		8
XC96002	4.5E-9	2.6E-10	t=6μm	33
XC96002	4.5E-9	8.8E-9	t=4μm	33
IDT3081	3E-11	0.9E-11		34

the K-5 part; it has not been applied to the data for the DSP. This is a more accurate method, but it does require additional fabrication details for a part, the type of information which microelectronics vendors are often unwilling to disclose.

VIII Conclusions

We have shown how the BGR method can be used in a number of different ways to calculate single event effect (SEE) rates and cross sections for protons and neutrons. The availability of the Weibull fit to provide an accurate and continuous functional representation of the heavy ion SEE cross section over LET is vital for the success of the method. Even when the Weibull data is from heavy ion testing of generic parts (rather than from the same lot of parts), the method is able to calculate proton/ neutron SEU cross sections to within a factor of 2-3 in most cases. Another feature of the method is the fact that even though it uses two parameters, t and C , the collection depth and efficiency, our experience indicates that specific values of t and C consistently give good agreement for a wide variety of different device types. We have shown that for SEU in recent parts, $t = 2 \mu\text{m}$ and $C=0.5$

works well for the Fig. 1 BGR functions, but for other BGR functions, different values of C and t may be needed. Further, for SEL in all except the most recent latchup-prone parts (proton SEL cross section $>1\text{E-}9 \text{ cm}^2$), $t=6\mu\text{m}$ and $C=1$ works well.

Regarding latchup, we indicate that in the testing of recent parts, proton-induced SEL cross section of $> 1\text{E-}9 \text{ cm}^2$ have been measured, and for these parts, $t=6\mu\text{m}$ does not work well. This is significant because it does not appear possible to know beforehand, based just on the heavy ion SEL cross section curve, when the standard BGR method (based on a minimum 6 μm recoil range) is applicable, or when a shorter minimum recoil range is needed to correctly predict the proton SEU cross section. It is not too surprising because the first data on a device exhibiting an unusually high proton-induced SEL cross section was only published a year ago. It does mean that there are limitations in using the BGR method for proton-induced SEL, since we cannot identify a priori from the heavy ion SEL cross section curve which parts have the very high susceptibility to SEL by protons and neutrons. For these latter parts, it appears that a smaller minimum recoil range is sufficient for the energy deposition to contribute to latchup, and when this adjustment is made, the model gives fair agreement.

REFERENCES

- 1) J. F. Ziegler and W. A. Lanford, "Effect of Cosmic Rays on Computer Memories," *Science*, **206**, 776 1979
- 2) J. R. Letaw and E. Normand, "Guidelines for Predicting Single Event Upsets in Neutron Environments," *IEEE Trans. Nucl. Sci.*, **NS-38**, 1500, 1991
- 3) P. Calvel, C. Barillot, P. Lamothe, R. Ecoffet, S. Duzellier and D. Falguere, "An Empirical Model for Predicting Proton Induced Upset," *IEEE Trans. Nucl. Sci.*, **43**, 2827, 1996
- 4) J. Barak, J. Levinson, A. Akkerman, Y. Lifshitz and M. Victoria, "A Simple Model for Calculating Proton Induced SEU," *IEEE Trans. Nucl. Sci.*, **43**, 979, 1996
- 5) R. A. Reed, P. J. McNulty, W. J. Beauvais, W. Abdel-Kader, E. Stassinopoulos and J. Barth, "A Simple Algorithm for Predicting Proton SEU Rates in Space Compared to the Rates Measured on the CRRES Satellite," *IEEE Trans. Nucl. Sci.*, **41**, 2389, 1994
- 6) P. J. Griffin, T. F. Luera, F. W. Sexton, P. J. Cooper, S. G. Karr, G. Hash and E. Fuller, "The Role of Thermal and Fission Neutrons in Reactor-Induced Upsets in Commercial SRAMs," *IEEE Trans. Nucl. Sci.*, **44**, 2079, 1997
- 7) P. J. McNulty, W. Beauvais and D. Roth, "Determination of SEU Parameters of NMOS and CMOS SRAMs," *IEEE Trans. Nucl. Sci.*, **38**, 1463, 1991
- 8) E. Normand, J. L. Wert, D. L. Oberg, P. P. Majewski, W. G. Bartholet, S. K. Davis, M. Shoga, S. A. Wender and A. Gavron, "Single Event Upset and Latchup Measurements in Avionics Devices Using the WNR Neutron Beam and a New Neutron-Induced Latchup Model," *Workshop Record, 1995 IEEE Radiation Effects Data Workshop*, p. 33

- 9) K. C. Chandler and T. W. Armstrong, "Operating Instruction for the High Energy Nucleon-Meson Transport Code, HETC," Report ORNL-4744, Oak Ridge National Lab, 1972
- 10) "Guidebook for the ENDF/B-V Nuclear Data Files," EPRI Report NP-2510, Brookhaven National Lab, 1982
- 11) E. L. Petersen, J. C. Pickel, J. H. Adams and E. C. Smith, "Rate Prediction for Single Event Effects," IEEE Trans. Nucl. Sci., **NS-39**, 1577 1992
- 12) E. Normand, "Single Event Effects in Avionics," IEEE Trans. Nucl. Sci., **43**, 461, (1996)
- 13) R. Velazco, S. Karoui and T. Chapius, "SEU Testing of 32-Bit Microprocessors," Workshop Record, IEEE Radiation Effects Data Workshop, 1992, p. 16; also "Heavy Ion Test Results for the 68020 Microprocessor and the 6882 Coprocessor," RADECS 91, Proceedings of the First European Conference on Radiation and its Effects on Devices and Systems, Montpellier, France, Sept. 1991
- 14) R. Katz, "Summary of Proton Test on the Actel RH1020 at Indiana University, June 1998," NASA-GSFC
- 15) R. Katz and K. LaBel, "Summary of Proton Test on the Actel A1280A at Indiana Univ., June 1998," NASA-GSFC
- 16) R. Katz, private communication
- 17) "SEU Proton Results (RH1280)," Actel Corp.
- 18) A. Taber and E. Normand, "Single Event Upset in Avionics," IEEE Trans. Nucl. Sci., **NS-40**, 120 1993
- 19) E. Normand, D. Oberg, J. Wert, J. Ness, S. Wender, P. Majewski, and A. Gavron, "Single Event Upset & Charge Collection Measurements Using High Energy Protons and Neutrons," IEEE Trans. Nucl. Sci., **41**, 2203 1994
- 20) E. Normand, "Single Event Upset at Ground Level," IEEE Trans. Nucl. Sci., **43**, 2742, 1996
- 21) J. E. Hewitt, L. Hughes, J. W. Baum, A. V. Kuehner, J. B. McCaslin, A. Rindi, A. Smith, L. Stephens, R. Thomas and C. G. Welles, "Ames Collaborative Study of Cosmic Ray Neutrons: Mid-Latitude Flights," Health Physics, **34**, 375, 1978
- 22) E. Fuller, private communication
- 23) T. M. Scott, "Cosmic Ray Upset Experiment Results," IBM Report, 89-PN6-023, November, 1989
- 24) S. Duzellier, R. Ecoffet, D. Falguere, T. Nuns, L. Guibert, W. Hajdas and M. Calvert, "Low Energy Proton Induced SEE in Memories," IEEE Trans. Nucl. Sci., **44**, 2306, 1997
- 25) K. Johansson, P. Dyreklev, B. Granbom, N. Olsson, J. Blomgren and P-U Renberg, "Energy-Resolved Neutron SEU Measurements from 22 to 160 MeV," paper presented at the 1998 IEEE NSREC, Newport Beach, CA, July, 1998
- 26) J. Barth, "Modeling Space Radiation Environments," 1997 IEEE NSREC Short Course, Snowmass Village, CO,
- 27) Space Radiation, Commercial software available from Space Radiation Associates, Eugene, OR
- 28) SSP 30512 Revision C, "Space Station Ionizing Radiation Design Environment," International Space Station Alpha, NASA, June, 1994
- 29) P. O'Neill and G. Badhwar, "Single Event Upsets for Space Shuttle Flights of New General Purpose Computer Memory Devices," IEEE Trans. Nucl. Sci., **41**, 1755, 1994
- 30) D. Falguere, S. Duzellier and R. Ecoffet, "SEE In-Flight Measurement on the MIR Orbital Station," IEEE Trans. Nucl. Sci., **41**, 2346, 1994
- 31) J. Levinson, A. Akkerman, M. Victoria, M. Hess, D. Ilberg, M. Alurralde, R. Henneck and Y. Lifshitz, "New Insights Into Proton Induced Latchup: Experiment and Modeling", Appl. Phys. Letters, **63**(21), 22, Nov. 1993
- 32) A. Johnston, G. M. Swift and L. D. Edmonds, "Latchup in Integrated Circuits from Energetic Protons," IEEE Trans. Nucl. Sci., **44**, 2367, 1997
- 33) P.M.O'Neill and W. X. Culpepper, private communication
- 34) J. R. Kimbrough, N. J. Collela, S. M. Denton, D. L. Schaeffer, D. Shih, J. Wilborn, P. G. Coakley, C. Casteneda, R. Koga, D. Clark and J. L. Ullman, "Single Event Effects and Performance Predictions for Space Applications of RISC Processors," IEEE Trans. Nucl. Sci., **41**, 2706, 1994
- 35) S. Duzellier, D. Falguere, and R. Ecoffet, "Heavy Ion/Proton Test Results on High Integrated Memories," Workshop Record, IEEE Radiation Effects Data Workshop, 1993, p. 36